

Computational Insights into Processes Underlying the Amine-Induced Fluorescence Quenching of a Stimuli-Responsive Phenol-Based Hexameric Foldamer Host

Chang Sun,[†] Ying Liu,[†] Jiaqiang Liu,[‡] Yu-Jing Lu,[‡] Lin Yu,[‡] Kun Zhang,[‡] and Huaqiang Zeng^{*,†,§}

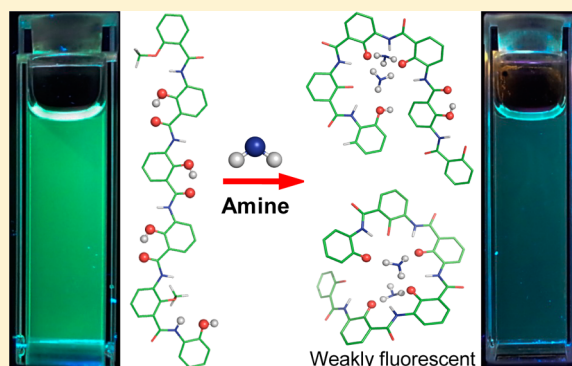
[†]Department of Chemistry, National University of Singapore, 3 Science Drive 3, Singapore 117543

[‡]Faculty of Chemical Engineering and Light Industry, Guang Dong University of Technology, Guang Dong, China 510006

[§]Institute of Bioengineering and Nanotechnology, 31 Biopolis Way, The Nanos, Singapore 138669

Supporting Information

ABSTRACT: Recently, we reported that amine-induced folding of a more fluorescent, more linear structure into less fluorescent, more curved or helically folded states enables patterned recognitions of amines and ammoniums. In this article, we have carried out extensive *ab initio* calculations at the B3LYP/6-31G level that not only map out the detailed amine-induced folding/quenching pathways and plausible folding/quenching species but also surprisingly reveal the binding of amines to anionic hosts to be unusually cooperative in a way that the progressively more charged anionic hosts act as increasingly better “amine trappers”. Accordingly amine-dependent folding occurs via a synergistic action of amines’ basicity and the progressively more curved backbone of the host. Although a hexamer carrying four deprotonable hydroxyl sites can reach a tetra-anionic state, mono-, di-, tri-, and tetra-anionic complexes likely dominate as the major quenching species in the presence of, respectively, 2, 4, 8, and 72 equiv of primary amines.



INTRODUCTION

Aromatic foldamers of diverse structures¹ endowed with various functions² have been demonstrated over the recent years. In particular, stimuli-responsive aromatic foldamers have attracted increasingly engendered attentions with structural transitions inducible³ by various stimuli including a change in concentration^{3b} or solvent polarity,^{3a} protonation,^{3c–e} light,^{3f–i} neutral guest molecules,^{3j} cations,^{3k,l} and anions,^{3m–q} as well as by a covalently linked macromolecule.^{3r} Although patterned recognition of amines and ammoniums can now be achieved by using a structurally rigid helically folded pyridine oligoamide host,^{2l} amines and ammoniums have not been explored previously to perturb the conformations of foldamer molecules.

Phenol oligoamides such as **1** and **2** have been recently shown to exhibit protonation/deprotonation-induced conformational switching, producing H-bonding patterns of two different types (Figure 1).^{3d} Such conformational preferences adopted by **1** and **2** can be further supported by *ab initio* calculations in our current investigation, demonstrating that the most stable conformers **1** and **2** are more stable than other alternative conformations of their respective categories by at least 3.41 and 17.47 kcal/mol (Figure 1). This early study backed up by our own *ab initio* calculations suggests that phenol groups make the phenol-based oligomeric backbone more linear and possibly more planar, while both phenolate and methoxybenzene result in a more curved or even helically

folded conformation. More specifically and as demonstrated recently by us and others, oligomers containing only methoxy groups and no hydroxyl groups are conformationally rigidified by inward-pointing intramolecular H-bonds of N–H...O type to take crescent, helically folded or circularly folded structures,⁴ while phenol-based oligoamides **3–7** containing up to four hydroxyl groups at various positions can be more linear (Figure 2a).⁵ For instance, although pentamer **3**⁵ was recently demonstrated by us to take a more linear geometry in solid state as shown in Figure 2b, transformation of the central OH group in **3** into an alkoxy group OMe via methylation induces **3** into a helical conformation.^{4e,f} Conversion of the same OH group into a phenolate moiety by deprotonation also results in a helical conformation (Figure 2c). Depending on the location and number of OH and OMe groups, these foldamer molecules can curve in two different directions as seen between **3/4** and **5/6** (Figure 2a). Consequently, their binding affinities toward amines/ammoniums and the corresponding energetic profiles underlying the binding process may differ from each other.

Moreover, these roughly planar molecules display very interesting conformation-dependent fluorescent properties in line with the relative linearity of hexameric backbones in **4–7**. These oligoamides are presented as a tree-like sketch drawing

Received: January 7, 2014

Published: March 7, 2014

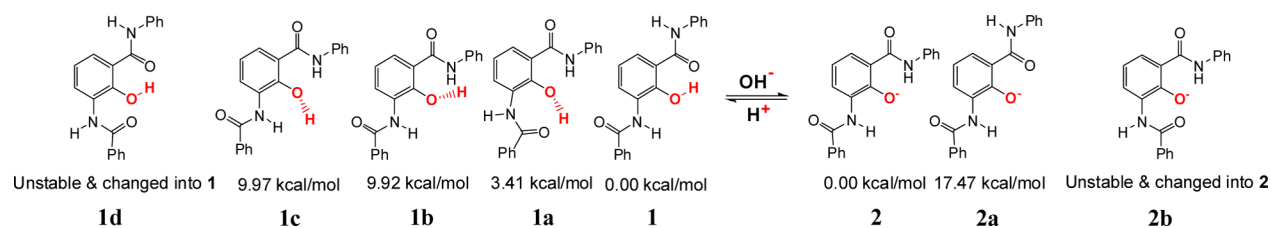


Figure 1. Deprotonation/protonation-promoted conformational switching between phenol-based oligoamides **1** and **2**. Both **1** and **2** are computationally shown to be the most stable conformers and more stable than others by 3.41 and 17.47 kcal/mol in their respective categories. Conformers **1d** and **2b** are unstable and, after geometrical optimizations, are conformationally changed into **1** and **2**, respectively.

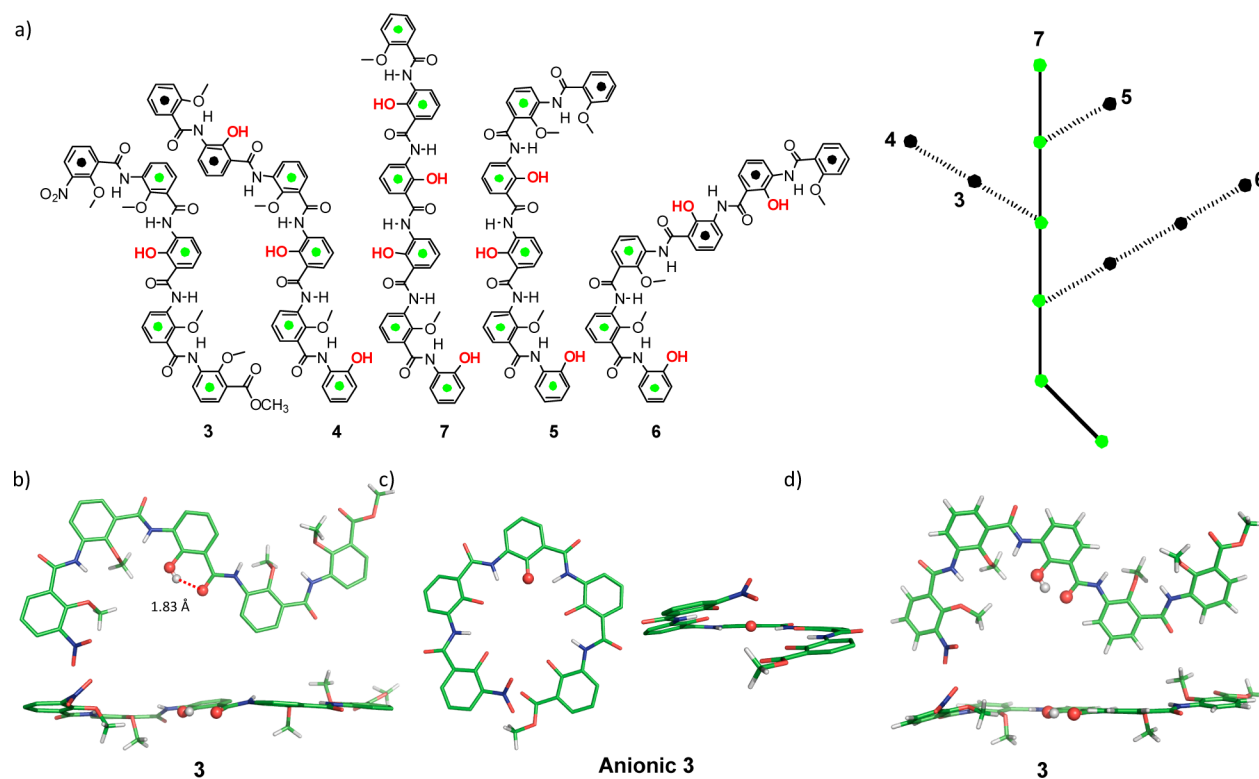


Figure 2. (a) Chemical structures of conformationally switchable fluorescent oligophenol foldamers **3–7** and a tree-like sketch representation of **3–7**, highlighting conformational similarity and differences among them. (b) Top and side views of crystal structure of pentamer **3**,⁵ demonstrating good planarity in backbones of **3–7** and the ability of the hydroxyl group in the red ball to form an alternative H-bonding pattern identical to that in **1** from Figure 1. Top and side views of *ab initio* calculated structure of (c) anionic **3** that becomes helically folded upon deprotonating the central hydroxyl group (O-atom in red ball) and (d) neutral **3** that looks remarkably similar to its crystal structure, demonstrating the high reliability of *ab initio* calculation at the B3LYP/6-31G level. The exteriorly arrayed aromatic protons in panels b–d and all the four interior methyl groups in panel c were removed for clarity of view. Oligophenols **3–7** contain from 1–4 hydroxyl groups and are conformationally sensitive to acid/base treatments.

counting from their hydroxyl (or ester for **3**) end to the methoxy (or nitro for **3**) end (Figure 2a). Accordingly, the more crescent-shaped structures such as **4–6** are less fluorescent than the more linear **7**.⁶ We thus envisioned that **4–7** containing deprotonable OH groups must be sensitive to the basicity of the solutions and should be able to undergo amine-induced folding, possibly allowing an easy detection or classification of amines and ammonium ions via changes in fluorescence intensity.

Very recently, we indeed demonstrated that with the use of guest molecules as simple as amines, carefully engineered and optimized phenol-based oligoamides such as hexamer **7** do undergo a dramatic structural change from a more linear geometry into a progressively more curved or eventually helically folded structure.⁵ These conformational changes result from a total of four hydroxyl-based acid/base-sensitive conformational switches at various locations. Concurrent with

this structural change, differential fluorescence quenchings of **7** by amines of various types were observed, allowing for the patterned recognition of amines and ammonium ions with the extent of fluorescence quenching increasing in the order of ammonium ions \approx tertiary amines $<$ acyclic secondary amines \approx branched primary amines $<$ nonbranched primary amines \approx cyclic secondary amines.⁵

The primary focus of this Article is on the use of *ab initio* calculations at the B3LYP/6-31G level to look into whether the amine-induced folding of hexamer **7** is a cooperative process and to deduce the plausible quenching pathways and quenching species underlying the processes that are consistent with the ¹H NMR data. This high level *ab initio* calculation has consistently allowed us to (1) predict the structures of a series of analogous H-bond-rigidified foldamer molecules that were verified experimentally later by their crystal structures,^{2b,f,j,4d–f,7} (2) rationalize the chemo- and regioselective demethylations

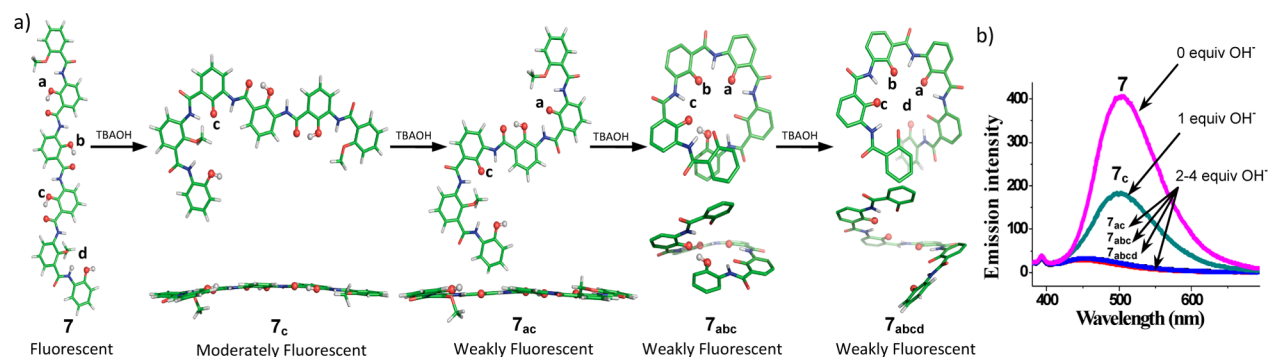


Figure 3. (a) TBAOH-promoted stepwise conformational switching involving **7** and its computationally determined most stable intermediate anionic isomers 7_c , 7_{ac} , 7_{abc} and 7_{abcd} by *ab initio* calculations at the B3LYP/6-31G level in THF. In 7_{abc} and 7_{abcd} the interior methoxy methyl groups and exterior aromatic protons were removed for clarity of view. Both **7** and 7_c are fluorescent, and the anionic 7_{ac} , 7_{abc} and 7_{abcd} all likely fluoresce very weakly. (b) Fluorescence quenching spectra of **7** at 10 μ M in THF in the presence of up to 4 equiv of strong organic base TBAOH for deprotonating hydroxyl groups.

mediated by TBACl/Br,⁸ and (3) understand the observed unusually short intermolecular Cl...Cl contacts of 2.524 Å in 1D chain of dichloromethane molecules.^{2k}

RESULTS AND DISCUSSION

Molecular Design and Fluorescence Properties.⁵ The phenol-based folding oligoamide **7** is conformationally rigidified by intramolecular H-bonds to take up a roughly planar, linear structure. Upon deprotonation of up to four hydroxyl groups at various positions in **7** by either amines or other strong organic bases such as tetrabutylammonium hydroxide (TBAOH), various more curved or eventually helically folded anionic structures may result. To facilitate the data presentation and discussion, letters a–d are used to denote the positions of hydroxyl groups in **7**, and their lower-cases signify the positions where deprotonation(s) occur (Figure 3a and Table 1). For example, 7_{abc} refers to the anionic oligomer where the three hydroxyl groups at positions a, b, and c are all deprotonated.

As compiled in Table 1, our *ab initio* computations at the level of B3LYP/6-31G show that deprotonation takes place preferentially in the order of c, a, b, and d, sequentially generating the most stable anionic isomers 7_c , 7_{ac} , 7_{abc} and 7_{abcd} in the presence of strong organic base TBAOH. This is because the high basicity of TBAOH makes it able to

completely deprotonate any phenolic hydroxyl group. Since 1 equiv of TBAOH can deprotonate only one hydroxyl group in **7**, addition of 2 equiv of TBAOH therefore deprotonates two hydroxyl groups in total, presumably producing dianionic 7_{ac} rather than trianionic 7_{abc} that requires 3 equiv of TBAOH. Further, 2 equiv of TBAOH likely will not be able to produce trianionic species at the detectable levels as formation of trianionic species will be accompanied by monoanionic species such as 7_c that is pretty fluorescent (Figure 3b). With respect to the starting conformation of hexamer **7** that is very linear, dianionic 7_{ac} has two highly curved substructures on its two ends, and contrary to our general observations, such structural changes, rather than a change in the degree of conjugation of the fluorophore, may possibly account for the observed spectral shift of ~50 nm in both Figures 3b and 4a. It should be noted, however, this relative order in deprotonation using TBAOH likely can be altered by structure-stabilizing guest molecules such as primary amines as will be elaborated later. This is because although TBAOH easily removes the hydroxyl protons, the three butyl substituents from cationic TBA⁺ prevents its positively charged N-atom from efficiently interacting with the phenolate O-atoms from anionic oligomers. From the computed structures, while the most stable anionic isomers 7_c and 7_{ac} adopt a planar crescent conformation, anionic 7_{abc} starts taking up a helical structure (Figure 3a). As shown recently by us,⁵ the fluorescence properties of **7** and these anionic versions are expected to follow the decreasing order of $7 > 7_a \approx 7_b \approx 7_c > 7_{ab} \approx 7_{bc} \approx 7_{ac} \approx 7_{abc} \approx 7_{abcd}$ where monoanionic oligomers are moderately fluorescent and di/tri/tetra-anionic oligomers are essentially nonfluorescent (Figure 3b).

Amine-Induced Folding and Fluorescence Quenching of Phenol-Based Foldamer **7.**⁵ In light of the above observations pointing to conformation-dependent fluorescence properties of **7**, amine-induced folding was monitored by fluorescence spectroscopy. Fluorescence measurements in THF using **7** show that **7** not only performs best for amine recognition among hexamers 4–7 but also allows for the patterned recognition of amines and ammoniums (Figure 4). Among amines of varying types, nonbranched primary amines (1-propyl amine, 1-butylamine, etc.) and cyclic secondary amines (azetidine, pyrrolidine, and piperidine) elicit the most fluorescence quenched of >80% for **7**, branched primary amines (e.g. isopropyl amine) and acyclic secondary amines result in fluorescence quenched of 65–70%, and tertiary amines and cyclic secondary amines containing additional

Table 1. Relative Stabilities of Varying Anionic Isomers^a Derived from **7^b**

Mono-anionic isomers with one phenolate anion (kcal/mol)					
7_a	7_b	7_c	7_d		
5.39	1.92	0.00	18.99		
Di-anionic isomers with two phenolate anions (kcal/mol)					
7_{ab}	7_{bc}	7_{ac}	7_{ad}	7_{bd}	7_{cd}
13.84	7.64	0.00	16.67	14.51	15.66
Tri-anionic isomers with three phenolate anions (kcal/mol)					
		7_{abc}	7_{abd}	7_{acd}	7_{bcd}
		0.00	11.77	5.50	13.37

^aAnionic oligomers can be generated by using organic bases such as TBAOH with their energies respectively normalized against the most stable isomers 7_c , 7_{ac} and 7_{abc} . ^bGeometrically optimized at the level of B3LYP/6-31G with single point energy calculated at the B3LYP/6-311+G(2d,p) level using THF as the implicit solvent.

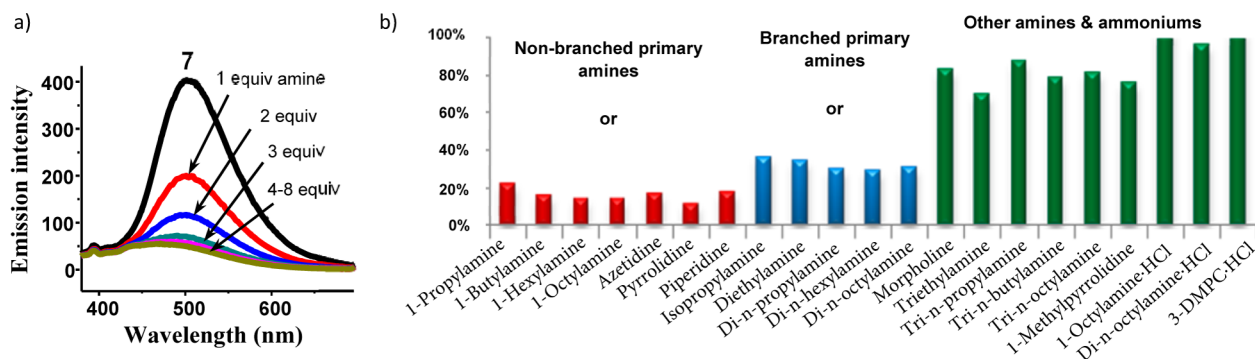


Figure 4. (a) Fluorescence quenching spectra of **7** by up to 8 equiv of 1-octylamine. (b) Patterned fluorescence quenching of **7** by 8 equiv of amines of various types. The fluorescence spectra/data were obtained at 10 μM concentration of **7** in THF containing 1% DMSO at room temperature with an excitation wavelength at 351 nm. DMPC = dimethylaminopropylchloride.

electron-withdrawing elements (e.g. morpholine) effect only a marginal quenching of 32% in the best scenario by triethylamine. Further testing of hexamer **7** against three ammonium salts (1-octylamine-HCl, di-*n*-octylamine-HCl, and 3-dimethylaminopropylchloride-hcl) demonstrates no detectable changes in the fluorescence intensity.

The facts that (1) the majority of amines studied herein have very similar $\text{p}K_{\text{a}}$ values and basicities, (2) secondary amines often are more basic than primary or tertiary amines, and (3) nonbranched primary amines and cyclic secondary amines elicit the most fluorescence quenching suggest that, after proton transfers from **7** to amine molecules, the efficient interaction between anionic **7** (e.g., 7_{c} , 7_{ac} , 7_{abc} , 7_{abcd} , etc.) and cationic amine guests via charge-assisted H-bonds, rather than their basicity, is the most important factor that induces the linear host into a more curved weakly fluorescent anionic structure by switching from H-bonding pattern as in **1** to that in **2** (Figure 1). Apparently, these charge-assisted H-bonds are dependent on the charge states of phenol-based host and amine guests as well as basicity and steric hindrance of amine guests. Accordingly, protonated nonbranched primary amines are able to stabilize anionic **7** in its various deprotonated states, leading to a large quenching in fluorescence. Likewise, cyclic amine with its alkyl substituents being tied back into a ring is held clear of the protonated amine group, allowing it to efficiently approach and stabilize anionic **7** without much hindrance. In contrast, despite having basicities similar to those of nonbranched primary amines and cyclic secondary amines, sterically more hindered branched primary amines, acyclic secondary amines, and tertiary amines in their protonated states are less able to bind and stabilize anionic **7**, thereby exerting less quenching effects. In the case of morpholine, introduction of one additional electron-withdrawing O-atom reduces its $\text{p}K_{\text{aH}}$ to 8.4 through an inductive effect, making it weakly basic and incapable of removing the hydroxyl proton from **7**. Ammonium salts are incapable of removing any hydroxyl proton from **7** either and thus unable to induce a noticeable conformational change in **7**.

Amine-Induced Folding/Quenching Pathways and Possible Folding/Quenching Species. The theoretical calculations at the B3LYP/6-31G level were further applied to **7** and its anionic analogues in the presence of amines. We will focus our attention on primary amines that elicit the most significant quenching to obtain insights into the amine-induced quenching mechanism, folding pathways, and structures of the complexes possibly responsible for the quenching. To simplify

the calculations, methylamine will be taken as the representative structural model for primary amines, and for every complex described below, up to 12 alternative conformations have been compared (Supplementary Figures S3–S23) in order to locate local minima, with the most stable ones presented in Figures 6–8 and Tables 1–4.

For neutral **7** in its linear conformation, its 1:1 complex with neutral methylamine surprisingly has a higher free energy than its unbound constituent parts. This indicates instability of the formed complexes, formation of which requires, rather than releases, energy of at least 5.67 kcal/mol that depends on how the methylamine approaches **7** from different positions in four patterns (Figure 5a). In the most stable complexes from their respective patterns as shown by solid arrows in varying colors that still turn out to be endothermic (Figure 5a), a significant change to the backbone planarity occurs that may explain why

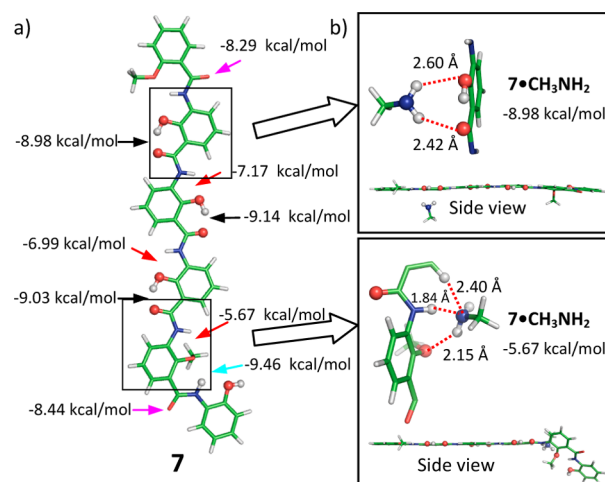


Figure 5. (a) *Ab initio* calculated binding energies absorbed when methylamine approaches neutral **7** from different positions in four patterns denoted as solid arrows in black, red, purple, and turquoise. (b, c) Side views of the most stable complexes formed between methylamine and **7** with negative binding energies of -8.98 and 5.67 kcal/mol from their respective patterns. In panel b, binding of methylamine to **7** planarizes the backbone of **7**, which may incur an energetic penalty and may explain why the complex formation is not an energetically favored process. In panel c, binding of methylamine to **7** distorts the backbone of **7** and forces two pairs of protons from amine and **7** to be in close proximity of 2.11 and 2.30 Å, both of which may incur an energetic penalty and may explain why the complex formation is an endothermic process.

the formation of both complexes is an energetically disfavored process. In the top complex (Figure 5b), the two amine protons form two intermolecular H-bonds of 2.60 and 2.42 Å with hydroxyl and amide O-atoms, respectively. The binding of amine to **7** planarizes the molecular backbone of otherwise more distorted **7** (Supplementary Figure S1a). In the bottom complex (Figure 5c), methylamine forms three intermolecular H-bonds of 1.84, 2.15, and 2.40 Å with amide N-atom, amide O-atom, and aromatic H-atom, respectively. The binding not only distorts the backbone of **7** but also forces the protons from the host and guest to come in very close proximity, creating two short repulsive H...H contacts of 2.11 and 2.30 Å that additionally destabilize the complex formation. The binding-induced backbone planarization or distortion to varying degrees is also seen when amine approaches **7** from other positions (Figure 5a).

As discussed above, among the three monoanionic oligomers, **7_c** is the most stable and should be formed preferentially over both **7_a** and **7_b** when treated with TBAOH that does not interact with and stabilize the anionic oligomer in its curved structure (Table 1). However, in the presence of structure-stabilizing molecules, i.e., amine in this case, binding of neutral or cationic methylamine molecules becomes more favored by, respectively, **7_c** and **7_b**, while a concurrent binding of one neutral and one cationic amine molecules is much more favored by **7_b** than by **7_c** (Table 2). This could be partially ascribed to the presence of a methoxy group around position c in anionic **7_c** (Figure 6), allowing it to bind only one guest molecule using the side not occupied by the methoxy methyl group. The thus formed complex **7_b**·(**CH₃NH₃⁺**+**CH₃NH₂**) (Figure 6a) is more

Table 2. Relative Stabilities and Binding Energies Underlying the Amine-Induced Conformational Switching Involving Mono-Anionic Isomers **7_a, **7_b**, and **7_c**^a**

n =	Mono-anionic Isomers		
	7_a	7_b	7_c
	Relative Stability (kcal/mol)		
n · CH₃NH₂	5.55	2.04	0.00
n · CH₃NH₃⁺	2.40	0.00	1.12
n ·(CH₃NH₃⁺ + CH₃NH₂)	5.74	0.00	5.76
	Binding Energy (kcal/mol)		
n + CH₃NH₂ → n · CH₃NH₂	-7.41	-3.90	-1.86
n + CH₃NH₃⁺ → n · CH₃NH₃⁺	14.05	12.99	9.95
n + CH₃NH₃⁺ + CH₃NH₂ → n ·(CH₃NH₃⁺ + CH₃NH₂)	15.27	17.54	9.86 ^b
7 + CH₃NH₂ → n · CH₃NH₃⁺	-5.46	-3.06	-4.18
7 +2 CH₃NH₂ → n ·(CH₃NH₃⁺ + CH₃NH₂)	-4.25	1.49	-4.27 ^b

^aGeometrically optimized at the level of B3LYP/6-31G with single point energy calculated at the B3LYP/6-311+G(2d,p) level using THF as the implicit solvent. A positive value in binding energy indicates an energetically favored exothermic binding event. ^bDue to the presence of a methoxy group, anionic **7_c** can bind only one guest molecule using the side not occupied by the methoxy methyl group; a concurrent binding of two guest molecules on two sides does not increase the stability of the formed complex **7_c**·(**CH₃NH₃⁺**+**CH₃NH₂**) with respect to complex **7_c**·**CH₃NH₃⁺**.

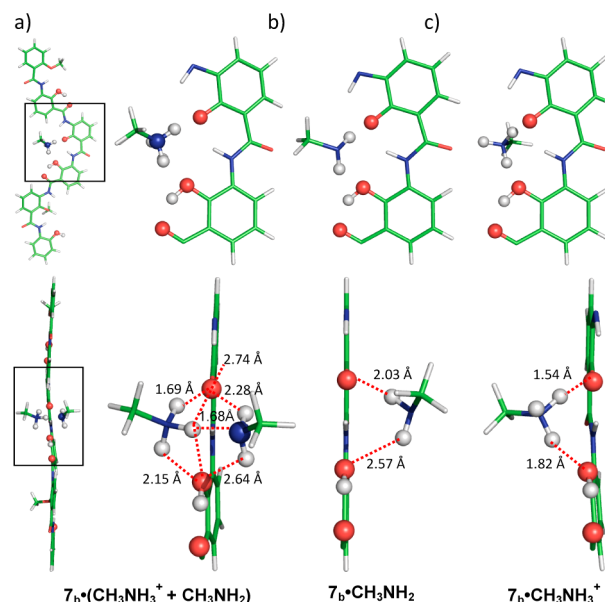


Figure 6. *Ab initio* calculated structures and the blowouts for complexes **7_b**·(**CH₃NH₃⁺**+**CH₃NH₂**), **7_b**·**CH₃NH₂**, and **7_b**·**CH₃NH₃⁺** arising from a respective binding of (a) one methylamine molecule and one cationic methylamine molecule, (b) one methylamine molecule, and (c) one cationic methylamine molecule to one molecule of anionic **7_b**. A positive cooperativity is clearly seen during the formation of **7_b**·(**CH₃NH₃⁺**+**CH₃NH₂**) with respect to **7_b**·**CH₃NH₂** and **7_b**·**CH₃NH₃⁺**. Likely, this may be due to the additional participation by one of the three protons from **CH₃NH₃⁺** in forming one strong intermolecular H-bond of 1.68 Å with the N-atom of **CH₃NH₂** and two weak H-bonds of 2.74 and of 2.81 Å with amide and hydroxyl O-atoms from **7_b**. In the top view of panel a, the two amine molecules superimpose on each other.

stable than complexes **7_a**·(**CH₃NH₃⁺**+**CH₃NH₂**) (Supplementary Figure S9) and **7_c**·(**CH₃NH₃⁺**+**CH₃NH₂**) (Supplementary Figure S10) by 5.74 and 5.76 kcal/mol, respectively. It is clear that a positive cooperativity exists in binding to two guest molecules by **7_b** and in forming complex **7_b**·(**CH₃NH₃⁺**+**CH₃NH₂**). By comparing the binding energies derived from binding of one methylamine (−3.90 kcal/mol), one cationic methylamine (12.99 kcal/mol), and one methylamine and one cationic methylamine (17.54 kcal/mol) by **7_b**, the positive cooperativity likely contributes an energy gain of 8.45 kcal/mol to the formation of **7_b**·(**CH₃NH₃⁺**+**CH₃NH₂**).

Such a positive cooperativity also operates during the binding of two methylamine molecules by neutral **7** to form the same complex of **7_b**·(**CH₃NH₃⁺**+**CH₃NH₂**) and estimatedly is worth at least 8.45 kcal/mol, which is equal to [1.49 − (−3.06) − (−3.90)] kcal/mol.⁹ Consistent with the experimental data on fluorescence quenching by primary amines, the binding of two methylamine molecules by one molecule of **7** is an exothermic process that releases energy of 1.49 kcal/mol, suggesting that amines can deprotonate the hydroxyl group in position b to generate less fluorescent anionic **7_b** and further stabilizes the resultant more curved conformation with regard to neutral **7**.

A careful examination of the computationally determined structures for complexes **7_b**·(**CH₃NH₃⁺**+**CH₃NH₂**) (Figure 6a), **7_b**·**CH₃NH₂** (Figure 6b), and **7_b**·**CH₃NH₃⁺** (Figure 6c) reveals the charged H-bonding, not the intrinsic basicity, to be the key factor that leads to the positive cooperativity. Despite slightly longer H-bonds formed in **7_b**·(**CH₃NH₃⁺**+**CH₃NH₂**) than those equivalents found in **7_b**·**CH₃NH₂** and **7_b**·**CH₃NH₃⁺**, an

additional participation by one of the three amine protons from CH_3NH_3^+ in forming one strong intermolecular H-bond of 1.68 Å with the N-atom of CH_3NH_2 and two weak H-bonds of 2.74 and 2.81 Å with amide and hydroxyl O-atoms from 7_b , affords a fully H-bonded caged structure. In this caged structure, the binding of cationic amine molecule to 7_b creates a higher-affinity binding pocket for the subsequent binding of neutral amine molecule or vice versa, producing a net positive cooperativity of 8.45 kcal/mol. This caged structure formed cooperatively is disfavored obviously by the sterically more hindered amines except for cyclic secondary amines and additionally by the weak H-bonding abilities in the case of tertiary amines.

As to dianionic oligomers, we will only consider their binding to cationic amines since (1) binding of anionic oligomers toward neutral amine molecules is much weaker than to cationic amines (see Table 2 as well as an exemplified comparison between the calculated *negative* binding energy of 4.22 kcal/mol for $7_{bc}\cdot\text{CH}_3\text{NH}_2$ and large *positive* binding energies of 18–23 kcal/mol for $n\cdot\text{CH}_3\text{NH}_3^+$ as shown in Table 3) and (2) production of one dianionic molecule (7_{ab} , 7_{bc} , or

Table 3. Relative Stabilities and Binding Energies Underlying the Amine-Induced Conformational Switching Involving Di-anionic Isomers 7_{ab} , 7_{bc} , and 7_{ac} ^a

n =	Di-anionic Isomers		
	7_{ab}	7_{bc}	7_{ac}
	Relative Stability (kcal/mol)		
$n\cdot\text{CH}_3\text{NH}_3^+$	3.32	0.00	4.35
$n\cdot 2\text{CH}_3\text{NH}_3^+$	1.09	0.00	5.77
	Binding Energy (kcal/mol)		
$7_{ac} + \text{CH}_3\text{NH}_3^+ \rightarrow n\cdot\text{CH}_3\text{NH}_3^+$	19.44	22.76	18.41
$7_{ac} + 2\text{CH}_3\text{NH}_3^+ \rightarrow n\cdot 2\text{CH}_3\text{NH}_3^+$	42.57	43.66	37.89
$7 + 2\text{CH}_3\text{NH}_2 \rightarrow n\cdot 2\text{CH}_3\text{NH}_3^+$	4.74	5.83	0.06

^aGeometrically optimized at the level of B3LYP/6-31G with single point energy calculated at the B3LYP/6-311+G(2d,p) level using THF as the implicit solvent. A positive value in binding energy indicates an energetically favored exothermic binding event.

7_{ac}) requires two molecules of methylamine for deprotonating the two hydroxyl groups in **7** and subsequently forms two cationic amine molecules that are more capable of occupying interior binding pockets in anionic oligomers than neutral amines. Similar to monoanionic oligomers, binding of one or two molecules of cationic methylamine alters the relative stabilities among the dianionic oligomers (Table 3). As a result, 7_{bc} , not 7_{ac} , forms the most stable amine complexes. A positive cooperativity for the formation of complexes $n\cdot 2\text{CH}_3\text{NH}_3^+$ seems to be operational for both 7_{ab} and 7_{ac} , but possibly not for 7_{bc} . A large binding energy of 22.76 kcal/mol associated with the binding of first cationic methylamine molecule to 7_{bc} makes a larger contribution to and results in the complex $7_{bc}\cdot 2\text{CH}_3\text{NH}_3^+$ being the most stable and more stable than those formed from 7_{ab} (Figure 7b) and 7_{ac} (Figure 7c) by 1.09 and 5.77 kcal/mol, respectively. Structurally, unlike a linear conformation taken up by dianionic 7_{ac} , dianionic 7_{bc} is crescent-shaped around its hydroxyl end, creating a cavity more suitable for hosting amine molecules (Figure 7a). In fact, the two cationic amine molecules can approach the host 7_{bc} from

both top and bottom sides to form a total of five strong intermolecular H-bonds with the shortest being 1.64 Å in length (Figure 7a). The top complex involving three intermolecular H-bonds of 1.71–2.17 Å is energetically more preferred by 1.94 kcal/mol over the bottom complex involving two intermolecular H-bonds, implying that complex $7_{bc}\cdot 2\text{CH}_3\text{NH}_3^+$ is formed more or less sequentially with the cationic amine molecules attacking first from the top side and then from the bottom. The formation of these very strong intermolecular H-bonds between host and guest molecules greatly stabilizes the crescent structure in dianionic 7_{bc} , allowing for the amine-induced induction of neutral **7** from its fluorescent linear conformation into a weakly fluorescent curved structure as in 7_{bc} and releasing an overall energy of 5.83 kcal/mol (Table 3).

Similar to 7_{bc} , dianionic 7_{ab} also contains a circularly folded interior cavity for favored recognition of cationic amines, and the binding energy between $7_{ab}\cdot 2\text{CH}_3\text{NH}_3^+$ and $7_{bc}\cdot 2\text{CH}_3\text{NH}_3^+$ differs slightly by 1.09 kcal/mol, suggesting these two weakly fluorescent complexes highly likely coexist in solution. Undoubtedly, the presence of a methoxy methyl group at either end in $7_{bc}\cdot 2\text{CH}_3\text{NH}_3^+$ and $7_{ab}\cdot 2\text{CH}_3\text{NH}_3^+$ disfavors the entering of branched amine molecules into the cavity, which is in accord with the experimentally observed trend in fluorescence quenching of **7** by amines of varying types (Figure 4).

Accompanying the formation of tri- and tetra-anionic oligomers 7_{abc} and 7_{abcd} via deprotonation by amines, three and four molecules of cationic amine are formed, respectively. Due to the fact that anionic 7_{abc} and 7_{abcd} are both helically folded to enclose a narrow 3D cavity of about 2.8 Å in radius and limited height (Figure 8),^{4e,f} a maximum of two cationic amine molecules can be bound by the cavity. Hence, the excessively generated cationic amine molecules (one for trianionic 7_{abc} and two for tetra-anionic 7_{abcd}) can associate only with exteriorly arrayed functional groups such as amide carbonyl O-atoms located along the backbone. Computationally, these exterior interactions produce estimated binding energies of 12–25 kcal/mol (see Figure 10d,e of the section Cooperative Binding Involving Amines and the Host). Subscripted symbols I and O refer to the location of the guest molecules, and under this designation, a complex such as $7_{abc}\cdot[(2\text{CH}_3\text{NH}_3^+)_I + (\text{CH}_3\text{NH}_3^+)_O]$ is a complex where its two cationic amine molecules are located inside the interior cavity with one cationic amine molecule exteriorly associating with the host 7_{abc} . Both $7_{abc}\cdot(2\text{CH}_3\text{NH}_3^+)_I$ and $7_{abcd}\cdot(2\text{CH}_3\text{NH}_3^+)_I$ contain very strong intermolecular H-bonds formed between phenolate O-atoms and cationic methylamine protons, and binding of two cationic amine molecules to the interior cavities of 7_{abc} and 7_{abcd} generates energies of 64.05 and 89.13 kcal/mol, respectively. By inclusion of respective energetic contributions of 16.58 and 42.93 kcal/mol resulting from the association of one or two cationic amine molecules with 7_{abc} at position C and with 7_{abcd} at positions B and C to form complexes $7_{abc}\cdot[(2\text{CH}_3\text{NH}_3^+)_I + (\text{CH}_3\text{NH}_3^+)_O]$ and $7_{abcd}\cdot[(2\text{CH}_3\text{NH}_3^+)_I + (2\text{CH}_3\text{NH}_3^+)_O]$ (Figure 10d,e), our calculations show that the overall processes inducing **7** into 7_{abc} or 7_{abcd} are both exothermic, respectively releasing energies of 5.18 or 10.14 kcal/mol (Table 4). Without considering the energy contribution from the exteriorly interacting cationic amines, all four processes, respectively inducing **7** into 7_{abc} , **7** into 7_{abcd} , 7_{bc} into 7_{abc} and 7_{abc} into 7_{abcd} , are endothermic and absorb energies of 11.40, 32.79, 17.23, and 37.98 kcal/mol. As

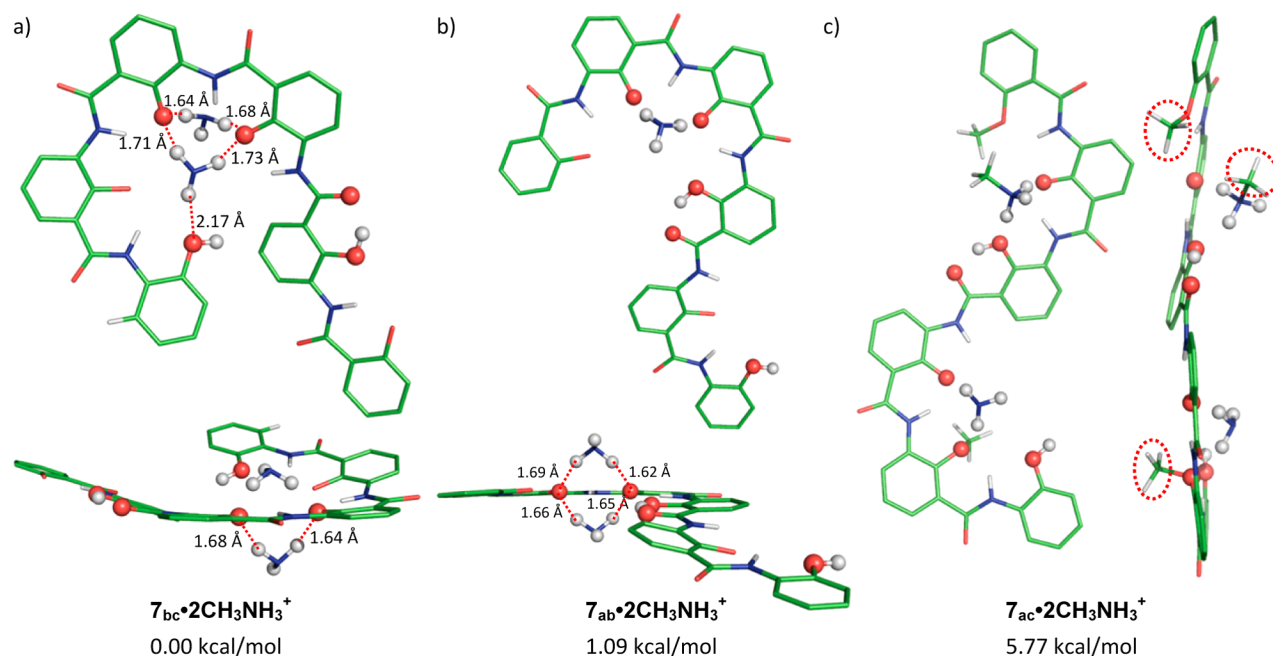


Figure 7. Top and side views of *ab initio* calculated structures for complexes (a) $7_{bc} \cdot 2\text{CH}_3\text{NH}_3^+$, (b) $7_{ab} \cdot 2\text{CH}_3\text{NH}_3^+$, and (c) $7_{ac} \cdot 2\text{CH}_3\text{NH}_3^+$ in the decreasing stability. In the top view of panel b, the two amine molecules superimpose on each other. For clarity of view, the exteriorly arrayed aromatic protons, methoxy groups, and methyl group of methylamine (a) and (b) were removed, and in panel c most of them were removed, leaving three of them in red dotted oval shapes to indicate the steric hindrance that prevents amine molecules from attacking from both sides of 7_{ac} .

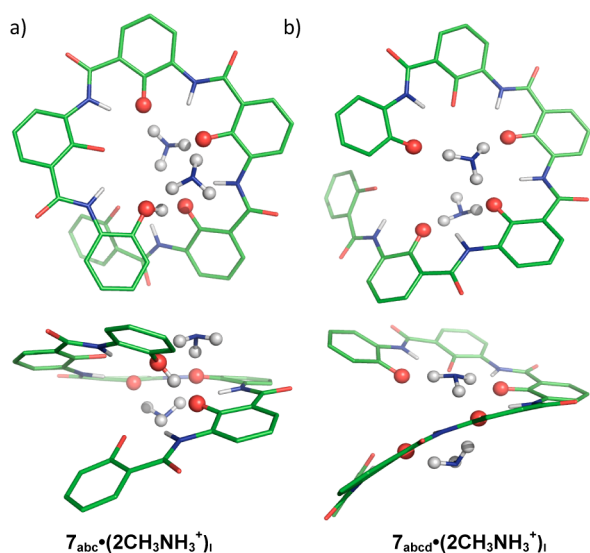


Figure 8. Top and side views of *ab initio* calculated helically folded structures for (a) $7_{abc} \cdot (2\text{CH}_3\text{NH}_3^+)_1$ and (b) $7_{abcd} \cdot (2\text{CH}_3\text{NH}_3^+)_1$. For clarity of view, the exteriorly arrayed aromatic protons, methoxy groups, and methyl group of methylamine were removed. Similar to other complexes, very strong intermolecular H-bonds are formed between anionic oligomers and cationic methylamine molecules.

elaborated in the subsequent section Cooperative Binding Involving Amines and the Host, although transforming the most stable dianionic complex $7_{bc} \cdot 2\text{CH}_3\text{NH}_3^+$ into trianionic complex $7_{abc} \cdot [(2\text{CH}_3\text{NH}_3^+)_1 + (\text{CH}_3\text{NH}_3^+)_0]$ consumes energy of 0.65 kcal/mol (Table 4), a further inclusion of up to four exteriorly interacting neutral amine molecules around the exterior of the trianionic complex at positions A, B, D, and E (Figure 10d) changes an otherwise endothermic process into a thermodynamically favored one, releasing energy of 3.98 kcal/mol (Table 4). Similarly, inclusion of three neutral amine

Table 4. Energetic Profiles Underlying the Amine-Induced Conformational Switching from Neutral 7 to Tri- and Tetra-anionic Isomers 7_{abc} and 7_{abcd} ^a

n =	Tri/Tetra-anionic oligomers	
	7_{abc}	7_{abcd}
Binding Energy (kcal/mol)		
$n + \text{CH}_3\text{NH}_3^+ \rightarrow n \cdot (\text{CH}_3\text{NH}_3^+)_1^b$	38.58	45.94
$n + 2\text{CH}_3\text{NH}_3^+ \rightarrow n \cdot (2\text{CH}_3\text{NH}_3^+)_1^b$	64.05	89.12
$n + \text{CH}_3\text{NH}_3^+ \rightarrow n \cdot (\text{CH}_3\text{NH}_3^+)_0^b$	16.58	24.86
$n + 2\text{CH}_3\text{NH}_3^+ \rightarrow n \cdot (2\text{CH}_3\text{NH}_3^+)_0^b$		42.93
$7 + 3\text{CH}_3\text{NH}_2 \rightarrow n \cdot [(2\text{CH}_3\text{NH}_3^+)_1 + (\text{CH}_3\text{NH}_3^+)_0]$	5.18 (9.81 ^c)	
$7 + 4\text{CH}_3\text{NH}_2 \rightarrow n \cdot [(2\text{CH}_3\text{NH}_3^+)_1 + (2\text{CH}_3\text{NH}_3^+)_0]$		10.14 (13.92 ^d)
$7_{bc} \cdot 2\text{CH}_3\text{NH}_3^+ + \text{CH}_3\text{NH}_2 \rightarrow n \cdot [(2\text{CH}_3\text{NH}_3^+)_1 + (\text{CH}_3\text{NH}_3^+)_0]$	-0.65 (3.98 ^c)	
$7_{abc} \cdot [(2\text{CH}_3\text{NH}_3^+)_1 + (\text{CH}_3\text{NH}_3^+)_0] + \text{CH}_3\text{NH}_2 \rightarrow n \cdot [(2\text{CH}_3\text{NH}_3^+)_1 + (2\text{CH}_3\text{NH}_3^+)_0]$		4.95 (8.73 ^d)

^aGeometrically optimized at the level of B3LYP/6-31G with single point energy calculated at the B3LYP/6-311+G(2,d,p) level using THF as the implicit solvent. A negative value in binding energy indicates an energetically disfavored endothermic binding event. ^bSubscript letters I and O symbolize the association of amine molecules with the host via interiorly or exteriorly arrayed O-atoms of the host. ^cThe energy contribution of 4.63 kcal/mol from the four amine molecules exteriorly interacting with trianionic host 7_{abc} at positions A, B, D, and E (Figure 10d) is included. ^dThe energy contribution of 3.78 kcal/mol from the three amine molecules exteriorly interacting with tetra-anionic host 7_{abcd} at positions A, C and D (Figure 10e) is included.

molecules around the exterior of tetra-anionic complex at positions A, D, and E (Figure 10e) makes the process more

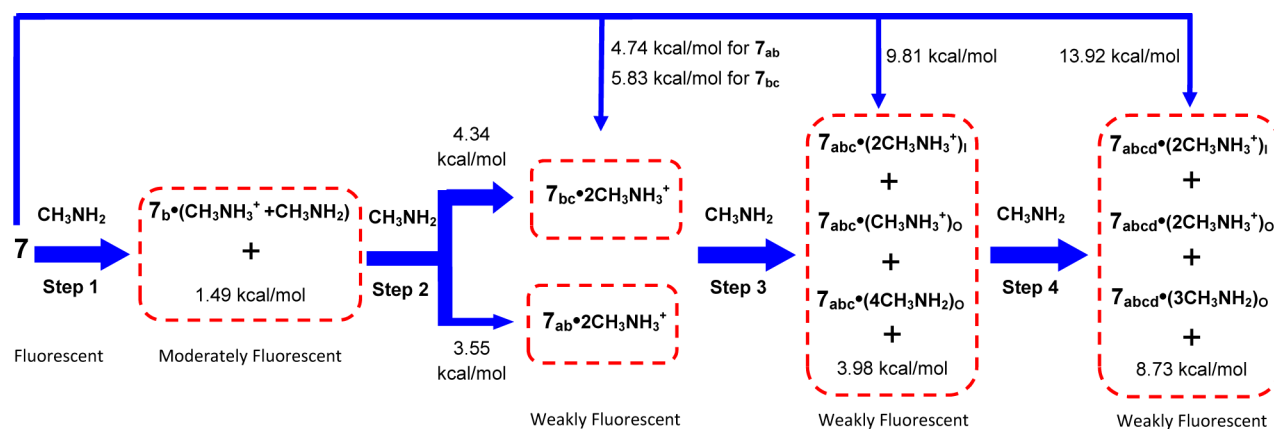


Figure 9. A schematic diagram that illustrates an amine-mediated four-step process, eventually leading to tetra-anionic complex 7_{abcd}^{\bullet} [$(2\text{CH}_3\text{NH}_3^+)_i + (2\text{CH}_3\text{NH}_3^+)_o + (3\text{CH}_3\text{NH}_2)_o$] from neutral 7 via intermediate oligomers and their complexes. In this sequential process, all four steps are thermodynamically favored, suggesting that anionic oligomers of varying types possibly coexist that depend on the amount of amine present in solution, collectively producing the quenching effect. The energy contributions from exteriorly interacting neutral and cationic amines as in tri- and tetra-anionic complexes in steps 3 and 4 contribute substantially to make the steps exothermic and afford helically folded anionic 7_{abc} and 7_{abcd} .

exothermic by 3.78 kcal/mol and releases a total energy of 8.73 kcal/mol.

Additional calculations reveal positive binding energies of 4.34 or 3.55 kcal/mol, respectively, for the single-step processes that lead to 7_{bc} or 7_{ab} from 7_b . Combining these values with the energy values in Tables 2–4 gives rise to a sound and complete picture of the overall four-step process, eventually yielding amine-induced helically folded tetra-anionic 7_{abcd} from neutral 7 in its linear structure via intermediate anionic oligomers (Figure 9). This stepwise process differs from that by using TBAOH (Figure 6) in that steps 1 and 2 respectively give rise to 7_b and $7_{bc}/7_{ab}$, rather than 7_c and 7_{ac} , as the most stable anionic oligomers through strong cooperative conformational changes¹⁰ in the presence of structure-stabilizing amine molecules. Further, all four individual steps are exothermic in free energy change, suggesting that all of the less fluorescent mono/di/tri/tetra-anionic oligomers could be the thermodynamically allowable fluorescence quenching species with their ratio sensitive to the amount of amines present in solution. Given a sufficient amount of amines and enough reaction time to equilibrate, the reaction may be possibly driven toward producing tetra-anionic complexes as the major quenching species (Figure 8b). Alternatively, considering that the pK_a value of the hydroxyl group at position d is considerably much higher than those at positions a–c^{3d} and that deprotonating hydroxyl proton d requires more energy of 13.60 kcal/mol than hydroxyl protons a–c (Table 1), in the presence of limited amounts of amines, amine molecules may not be able to remove hydroxyl proton d. In this scenario, the likely dominant quenching species may turn out to be tri- rather than tetra-anionic complexes (Figure 8a). The presence of either tri- or tetra-anionic complexes as major quenching species is consistent with the experimental ¹H NMR data compiled in Figure 11.

Cooperative Binding Involving Amines and the Host.

During our mechanistic calculations aimed at elucidating the possible quenching species and pathways, we unexpectedly found that the binding between amines and the host via exterior amide carbonyl O-atoms highly depends on the backbone linearity and charged state of the host even though such binding is already perceptibly position-dependent. What is unusual is that the binding mostly becomes more and more

cooperative and increases progressively and substantially in the order of neutral < mono- < di- < tri- < tetra-anionic states with a few exceptions happening to 7_b and 7_{bc} complexes (Figure 10). For instance, binding of one cationic amine molecule to the host in its neutral, mono-, di-, tri-, and tetra-anionic states via the exterior amide carbonyl O-atom at position E increasingly releases energies of -0.31 , 7.91, 9.10, 12.56, and 20.46 kcal/mol (Figure 10); the corresponding energies for binding of one neutral amine molecule at the same position E are -8.44 , 0.69, 0.71, 1.37, and 2.23 kcal/mol (Figure 10). These trends are consistently seen to a large extent in other positions where hydroxyl groups have been deprotonated to make amide carbonyl O-atoms accessible for binding by either neutral or cationic amines. Noticeably, position C appears to be the most favored binding site for cationic amines among all of the four types of anionic hosts, and helically folded 7_{abc} and 7_{abcd} interact with both neutral and cationic amines more strongly than partially folded 7_b and 7_{bc} (Figure 10d,e vs b,c). Moreover, tetra-anionic 7_{abcd} binds better to amines than trianionic 7_{abc} among all the positions A–E.

Such positive cooperativity is also operational during the binding of cationic amines to the anionic hosts via interior phenolate O-atoms. Hence, the largest binding energy from binding of one cationic amine to one anionic host of their own category increases in the same order of mono- < di- < tri- < tetra-anionic oligomers and measures, respectively, 14.05 (Table 2), 22.76 (Table 3), 38.58, and 45.94 kcal/mol (Table 4).

Apparently, these strongly cooperative interactions among amines and anionic hosts via both interior phenolate and exterior amide carbonyl O-atoms can well compensate for the large amount of energy needed to deprotonate the hydroxyl groups at varying positions and make all the processes outlined in Figure 9 exothermic that produce weakly fluorescent anionic complexes, accounting for the observed fluorescence quenching of host 7 .

Deducing Folding/Quenching Species by ¹H NMR and Molecular Modeling. Computationally as described above, tetra-anionic complexes could be the major quenching species. Given the much larger pK_a value of hydroxyl group at position d versus those at the other three positions a–c, trianionic complexes are more likely to be the predominant quenching

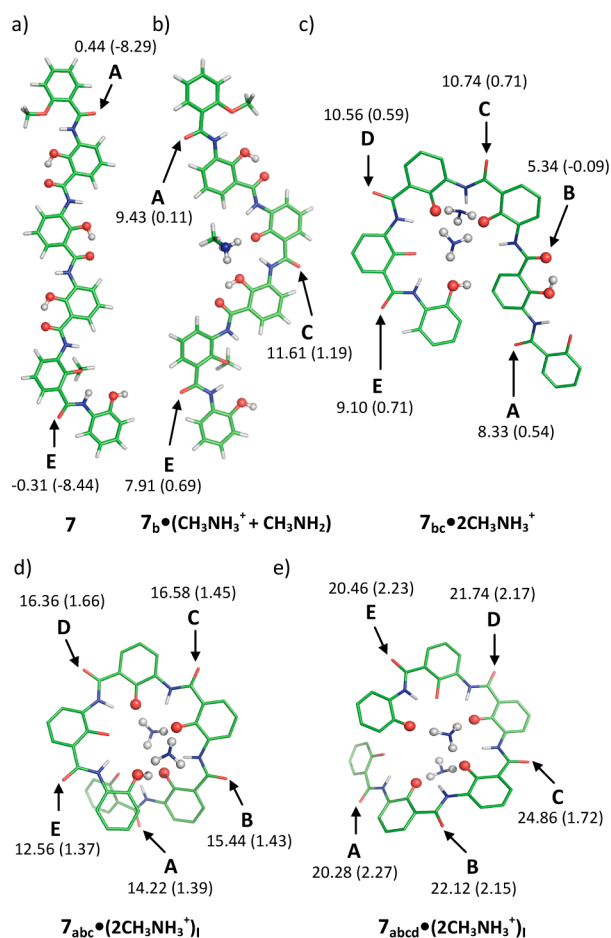


Figure 10. Computationally determined binding energies in kcal/mol arising from the binding of one cationic or neutral (values in bracket) methylamine molecule to host **7** in (a) neutral and (b) mono-, (c) di-, (d) tri-, and (e) tetra-anionic states via exterior amide carbonyl O-atoms at positions A–E. Binding toward carbonyl O-atoms adjacent to hydroxyl groups in panels a and b is much weaker and are not shown. This can be seen by comparing B with others in panel c.

species particularly in the presence of limited amounts of amines. To further clarify this, ^1H NMR studies were carried out in fully deuterated DMSO due to a poor solubility of **7** in CDCl_3 or $\text{THF}-d_8$.

Fluorescence investigations were first performed to confirm the amine-induced quenching can be similarly effected in DMSO. Addition of up to 8 equiv of 1-octylamine into **7** in DMSO indeed quenches the fluorescence intensity of **7** by 93%, a value similar to 87% quenching caused by the same amine in THF. By carefully comparing ^1H NMR spectra of **7** at 5 mM in DMSO in the presence of up to 4 equiv of strong base TBAOH (Figure 11b) with those obtained by treating **7** with up to 8 equiv of 1-octylamine (Figure 11c) and aided further by using the assignment of anionic oligomers in Figure 3, it can be seen that stepwise additions of up to 8 equiv of amine gradually transform the anionic intermediates accounting for the fluorescence of **7** (Figure 11c). Further addition of 64 equiv of amine eventually converts monoanionic 7_b to tetra-anionic 7_{abcd} as the predominant anionic species in the reaction via dianionic 7_{bc} and trianionic 7_{abc} as the intermediate anionic oligomers (Figure 11c).¹¹

In more detail as shown in Figure 11c, the first 2 equiv of amine likely afford complex $7_b \cdot (\text{CH}_3\text{NH}_3^+ + \text{CH}_3\text{NH}_2)$ (for its

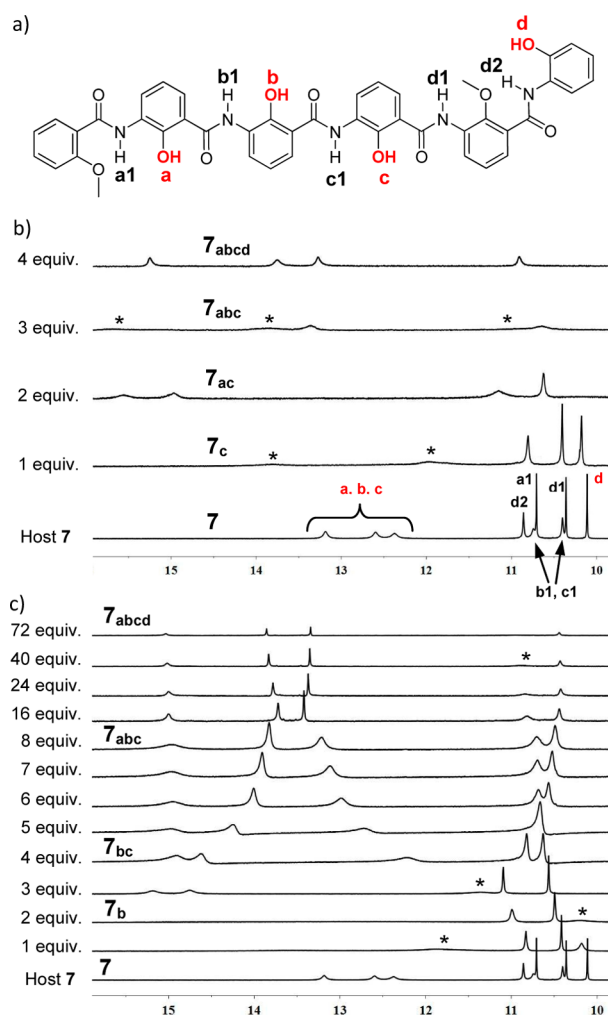


Figure 11. (a) Chemical structure of host **7**. (b, c) Description of the ^1H NMR spectra of **7** at 5 mM in $\text{DMSO}-d_6$ in the presence of 0–4 equiv of TBAOH and 0–72 equiv of 1-octylamine, respectively. All peaks in the presence of ≥ 4 equiv of amine belong to the amide protons.¹¹ The assignments of anionic hosts in panel b is based on the computational results in Table 1. The anionic hosts in panel c are assigned by comparing the spectra in panel c with those in panel b. These anionic hosts are the possible dominant quenching species that coexist with other minor ones in solution. The barely visible broad peaks are marked by asterisks (*).

structure, see Figure 6b) with the second 2 equiv of amine leading to dianionic $7_{bc} \cdot 2\text{CH}_3\text{NH}_3^+$ (for its structure, see Figure 7a). The subsequent addition of up to 4 equiv of amine produces an increasing amount of trianionic complexes $7_{abc} \cdot [(\text{2CH}_3\text{NH}_3^+)_1 + (\text{CH}_3\text{NH}_3^+)_0 + (m\text{CH}_3\text{NH}_2)_0]$ that eventually takes over $7_{bc} \cdot 2\text{CH}_3\text{NH}_3^+$ and that contains one cationic amine molecule at position C and up to $m = 4$ neutral amine molecules exteriorly interacting with the trianionic host 7_{abc} at the remaining four positions.¹² A final addition of sufficiently enough such as 64 equiv of amine molecules deprotonates the last hydroxyl proton d and converts trianionic to tetra-anionic complexes $7_{abcd} \cdot [(\text{2CH}_3\text{NH}_3^+)_1 + (\text{2CH}_3\text{NH}_3^+)_0 + (m\text{CH}_3\text{NH}_2)_0]$ where $m = 0$ –3 and cationic amines likely take up positions B and C (Figure 8b). It is worth mentioning that (1) both mono- and dianionic complexes are unlikely to have exteriorly interacting neutral amine molecules since such interactions are unfavored for the former (Figure 5a) and barely exothermic for the latter (Figure 10b), and (2) more

negatively charged anionic hosts such as 7_{abc} are more able to keep hold of both neutral and cationic amines than less anionic hosts such as 7_{bc} such that, in the presence of limited amounts of amines, 7_{abc} can have up to five exteriorly interacting amines at positions A–E while 7_{bc} may have none. Another important “take home message” that needs to be re-emphasized here is that without considering the substantial energy contributions from exteriorly interacting cationic amine molecules via amide carbonyl O-atoms as outlined in Figure 10d,e, both processes inducing neutral **7** into tri- or tetra-anionic states are endothermic (–17.23 and –37.98 kcal/mol, respectively), reflecting significant amounts of energy needed to deprotonate the last two hydroxyl protons c and d. Inclusion of these exterior interactions nevertheless makes the two processes thermodynamically allowable (Table 4), a perspective finding that is in line with the ^1H NMR results (Figure 11).

CONCLUSION

A modularly tunable strategy for amine sensing was recently demonstrated by us, leading to a new class of phenol-based fluorescent folding molecules with their backbones rigidified by intramolecular H-bonds and with their ability to fluoresce roughly in good correlation with their backbone linearity. By using strong organic bases such as TBAOH that deprotonates hydroxyl groups at four different locations in a stepwise manner, a four-step sequential folding of a more fluorescent linear structure into an essentially nonfluorescent helically folded tetra-anionic state via mono-, di-, and trianionic intermediates can be achieved (Figure 3a). However, the moderately strong organic bases in its limited presence can only realize a partial contraction of the initial extended linear conformation, resulting in less fluorescent, more curved mono-, di-, and trianionic oligomeric intermediates. Although the initial binding between amines and neutral host is very unfavored, the ability of progressively more charged anionic hosts to exhibit increasingly enhanced binding affinities toward both neutral and cationic amines allows 8 equiv of amines to produce the trianionic complex as the major quenching species in solution that contains two cationic amine molecules in its interior with one cationic and four neutral amine molecules exteriorly interacting with the trianionic host via amide carbonyl O-atoms. In contrast, the tetra-anionic complex seems to be the predominant quenching species in the presence of 72 equiv of amines. Interestingly, due to the strong ability of *in situ* produced cationic amine molecules to stabilize the otherwise less stable mono- and dianionic oligomers (7_b and 7_{bc}) via high strength charged H-bonding networks in a cooperative manner, 7_b and 7_{bc} become the more stable and predominant species in solution through strong cooperative conformational changes.¹⁰ These intermediates differ from those more stable mono- and dianionic 7_c and 7_{ac} generated by TBAOH and lead to diminished fluorescence intensities. Importantly, such ability to stabilize varying anionic oligomers that determine the extent of amine-mediated conformational switching works cooperatively, varies among the amines of different types, and is affected significantly more by H-bonding capabilities of the amines and their alkyl substituents than their intrinsic basicities. As such, nonbranched primary amines and cyclic secondary amines produce mono-, di-, and trianionic crescent-shaped oligomers to the largest extent, followed by branched primary amines and acyclic secondary amines with both tertiary amines and ammonium ions to the least, concurrently making possible the patterned recognition of varying amines and ammonium

ions by phenol-based foldamer molecules. In connection with the recently elucidated diverse functions by the H-bonded aromatic foldamers of varying types,^{1,2} it is quite unusual to note that these foldamer molecules, however, have not been applied to explore molecular recognition of functional groups as simple as amines.²¹ The approach described here may promise more selective recognitions of amines by other analogous conformationally switchable phenol-based foldamers with elongated backbones and/or with the replacement of methoxy groups by other bulkier groups at the two ends. This study further highlights the power of *ab initio* computations at the level of B3LYP/6-31G in yielding novel structural and mechanistic insights into the possible folding/quenching species and folding/quenching pathways that are in good accord with the experimental data.

ASSOCIATED CONTENT

Supporting Information

Description of *ab initio* molecular modeling, energies and Cartesian coordinates of computationally optimized structures listed in Tables 1–4 and Figures 5 and 10, other computationally determined structures, complexes and binding energies, 2D ^1H – ^{15}N HMQC and ^1H – ^1H ROESY spectra. This material is available free of charge via the Internet at <http://pubs.acs.org>.

AUTHOR INFORMATION

Corresponding Author

*E-mail: chmzh@nus.edu.sg; hqzeng@ibn.a-star.edu.sg

Notes

The authors declare no competing financial interest.

ACKNOWLEDGMENTS

Financial supports of this work to H.Z. by NRF CRP (R-154-000-529-281), SPORE (COY-15-EWI-RCFSA/N197-1), and NUS AcRF Tier 1 grants (R-143-000-534-112) and to Y.J.L. by National Natural Science Foundation of China (Grant 21102021)

REFERENCES

- (1) For some recent reviews in foldamer, see: (a) Gellman, S. H. *Acc. Chem. Res.* **1998**, *31*, 173. (b) Gong, B. *Acc. Chem. Res.* **2008**, *41*, 1376. (c) Saraogi, I.; Hamilton, A. D. *Chem. Soc. Rev.* **2009**, *38*, 1726. (d) Zhang, D.-W.; Zhao, X.; Hou, J.-L.; Li, Z.-T. *Chem. Rev.* **2012**, *112*, 5271. (e) Fu, H. L.; Liu, Y.; Zeng, H. Q. *Chem. Commun.* **2013**, *49*, 4127. (f) Ong, W. Q.; Zeng, H. Q. *J. Incl. Phenom. Macrocycl. Chem.* **2013**, *76*, 1.
- (2) For binding of metal ions, organic ions and small guest molecules by functional aromatic foldamers, see: (a) Qin, B.; Ren, C. L.; Ye, R. J.; Sun, C.; Chiad, K.; Chen, X. Y.; Li, Z.; Xue, F.; Su, H. B.; Chass, G. A.; Zeng, H. Q. *J. Am. Chem. Soc.* **2010**, *132*, 9564. (b) Ren, C. L.; Maurizot, V.; Zhao, H. Q.; Shen, J.; Zhou, F.; Ong, W. Q.; Du, Z. Y.; Zhang, K.; Su, H. B.; Zeng, H. Q. *J. Am. Chem. Soc.* **2011**, *133*, 13930. (c) Du, Z. Y.; Ren, C. L.; Ye, R. J.; Shen, J.; Lu, Y. J.; Wang, J.; Zeng, H. Q. *Chem. Commun.* **2011**, *47*, 12488. (d) Sanford, A. R.; Yuan, L.; Feng, W.; Yamato, K.; Flowers, R. A.; Gong, B. *Chem. Commun.* **2005**, 4720. (e) Ong, W. Q.; Zhao, H. Q.; Fang, X.; Woen, S.; Zhou, F.; Yap, W. L.; Su, H. B.; Li, S. F. Y.; Zeng, H. Q. *Org. Lett.* **2011**, *13*, 3194. (f) Zhao, H. Q.; Ong, W. Q.; Fang, X.; Zhou, F.; Hii, M. N.; Li, S. F. Y.; Su, H. B.; Zeng, H. Q. *Org. Biomol. Chem.* **2012**, *10*, 1172. (g) Hou, J.-L.; Yi, H.-P.; Sha, X.-B.; Li, C.; Wu, Z.-Q.; Jian, X.-K.; Wu, L.-Z.; Tung, C.-H.; Li, Z.-T. *Angew. Chem., Int. Ed.* **2006**, *45*, 796. (h) Jiang, H.; Leger, J. M.; Guionneau, P.; Huc, I. *Org. Lett.* **2004**, *6*, 2985. (i) Shirude, P. S.; Gillies, E. R.; Ladame, S.; Godde, F.; Shin-Ya, K.; Huc, I.; Balasubramanian, S. *J. Am. Chem. Soc.* **2007**, *129*, 11890. (j) Zhao, H. Q.; Ong, W. Q.; Zhou, F.; Fang, X.; Chen, X. Y.; Li, S. F.

Y.; Su, H. B.; Cho, N.-J.; Zeng, H. Q. *Chem. Sci.* **2012**, *3*, 2042. (k) Zhou, F.; Fu, H. L.; Ong, W. Q.; Ye, R. J.; Yuan, W. X.; Lu, Y.-J.; Huo, Y.-P.; Zhang, K.; Su, H. B.; Zeng, H. Q. *Org. Biomol. Chem.* **2012**, *10*, 5525. (l) Ong, W. Q.; Zhao, H. Q.; Sun, C.; Wu, J. E.; Wong, Z. C.; Li, S. F. Y.; Hong, Y. H.; Zeng, H. Q. *Chem. Commun.* **2012**, *48*, 6343. (m) Zhao, H. Q.; Shen, J.; Guo, J. J.; Ye, R. J.; Zeng, H. Q. *Chem. Commun.* **2013**, *49*, 2323.

(3) For stimuli-responsive foldamers, see: (a) Nelson, J. C.; Saven, J. G.; Moore, J. S.; Wolynes, P. G. *Science* **1997**, *277*, 1793. (b) Corbin, P. S.; Zimmerman, S. C. *J. Am. Chem. Soc.* **2000**, *122*, 3779. (c) Dolain, C.; Maurizot, V.; Huc, I. *Angew. Chem., Int. Ed.* **2003**, *42*, 2738. (d) Kanamori, D.; Okamura, T. A.; Yamamoto, H.; Ueyama, N. *Angew. Chem., Int. Ed.* **2005**, *44*, 969. (e) Hu, H. Y.; Xiang, J. F.; Yang, Y.; Chen, C. F. *Org. Lett.* **2008**, *10*, 1275. (f) Khan, A.; Kaiser, C.; Hecht, S. *Angew. Chem., Int. Ed.* **2006**, *45*, 1878. (g) Tie, C.; Gallucci, J. C.; Parquette, J. R. *J. Am. Chem. Soc.* **2006**, *128*, 1162. (h) Hua, Y.; Flood, A. H. *J. Am. Chem. Soc.* **2010**, *132*, 12838. (i) Wang, Y.; Bie, F.; Jiang, H. *Org. Lett.* **2010**, *12*, 3630. (j) Tanatani, A.; Hughes, T.; Moore, J. S. *Angew. Chem., Int. Ed.* **2002**, *41*, 325. (k) Barboiu, M.; Lehn, J.-M. *Proc. Natl. Acad. Sci. U.S.A.* **2002**, *99*, 5201. (l) Stone, M. T.; Moore, J. S. *J. Am. Chem. Soc.* **2005**, *127*, 5928. (m) Li, Y.; Flood, A. H. *J. Am. Chem. Soc.* **2008**, *130*, 12111. (n) Meudtner, R. M.; Hecht, S. *Angew. Chem., Int. Ed.* **2008**, *47*, 4926. (o) Wang, Y.; Li, F.; Han, Y.; Wang, F.; Jiang, H. *Chem.—Eur. J.* **2009**, *15*, 9424. (p) Suk, J.-m.; Naidu, V. R.; Liu, X.; Lah, M. S.; Jeong, K.-S. *J. Am. Chem. Soc.* **2011**, *133*, 13938. (q) Shi, Z.-M.; Chen, S.-G.; Zhao, X.; Jiang, X.-K.; Li, Z.-T. *Org. Biomol. Chem.* **2011**, *9*, 8122. (r) Ghosh, K.; Moore, J. S. *J. Am. Chem. Soc.* **2011**, *133*, 19650.

(4) (a) Yi, H. P.; Li, C.; Hou, J. L.; Jiang, X. K.; Li, Z.-T. *Tetrahedron* **2005**, *61*, 7974. (b) Yi, H.-P.; Wu, J.; Ding, K.-L.; Jiang, X.-K.; Li, Z.-T. *J. Org. Chem.* **2007**, *72*, 870. (c) Lu, Y.-X.; Shi, Z.-M.; Li, Z.-T.; Guan, Z. *Chem. Commun.* **2010**, *46*, 9019. (d) Qin, B.; Chen, X. Y.; Fang, X.; Shu, Y. Y.; Yip, Y. K.; Yan, Y.; Pan, S. Y.; Ong, W. Q.; Ren, C. L.; Su, H. B.; Zeng, H. Q. *Org. Lett.* **2008**, *10*, 5127. (e) Yan, Y.; Qin, B.; Shu, Y. Y.; Chen, X. Y.; Yip, Y. K.; Zhang, D. W.; Su, H. B.; Zeng, H. Q. *Org. Lett.* **2009**, *11*, 1201. (f) Yan, Y.; Qin, B.; Ren, C. L.; Chen, X. Y.; Yip, Y. K.; Ye, R. J.; Zhang, D. W.; Su, H. B.; Zeng, H. Q. *J. Am. Chem. Soc.* **2010**, *132*, 5869. (g) Qin, B.; Ong, W. Q.; Ye, R. J.; Du, Z. Y.; Chen, X. Y.; Yan, Y.; Zhang, K.; Su, H. B.; Zeng, H. Q. *Chem. Commun.* **2011**, *47*, 5419. (h) Qin, B.; Sun, C.; Liu, Y.; Shen, J.; Ye, R. J.; Zhu, J.; Duan, X.-F.; Zeng, H. Q. *Org. Lett.* **2011**, *13*, 2270. (i) Qin, B.; Shen, S.; Sun, C.; Du, Z. Y.; Zhang, K.; Zeng, H. Q. *Chem. Asian J.* **2011**, *6*, 3298. (j) Liu, Y.; Qin, B.; Zeng, H. Q. *Sci. China Chem.* **2012**, *55*, 55. (k) Fu, H. L.; Chang, H.; Shen, J.; Yu, L.; Zhang, K.; Zeng, H. Q. *Chem. Commun.* **2014**, *50*, 3582.

(5) Sun, C.; Ren, C. L.; Wei, Y. C.; Qin, B.; Zeng, H. Q. *Chem. Commun.* **2013**, *49*, 5307.

(6) We believe that the fluorescence properties of those nonhelically shaped oligophenols possibly are more sensitive to the backbone linearity than to the planarity. For a helically folded backbone, it is possible that both linearity and planarity play important roles for the observed fluorescence quenching of these conformationally switchable molecules. Further, hydroxyl groups may play a dual role in enhancing the fluorescence properties of the molecules: they directly participate in the fluorescence generation by linearizing the backbone and by its electron-rich nature. However, it is impossible to separate the effect of OH groups from the effect of backbone linearity on the fluorescence quenching. This is because deprotonation of OH groups is always accompanied by a concurrent reduction in backbone linearity.

(7) (a) Ong, W. Q.; Zhao, H. Q.; Du, Z. Y.; Yeh, J. Z. Y.; Ren, C. L.; Tan, L. Z. W.; Zhang, K.; Zeng, H. Q. *Chem. Commun.* **2011**, *47*, 6416. (b) Ren, C. L.; Zhou, F.; Qin, B.; Ye, R. J.; Shen, S.; Su, H. B.; Zeng, H. Q. *Angew. Chem., Int. Ed.* **2011**, *50*, 10612.

(8) (a) Qin, B.; Jiang, L. Y.; Shen, S.; Sun, C.; Yuan, W. X.; Li, S. F. Y.; Zeng, H. Q. *Org. Lett.* **2011**, *13*, 6212. (b) Du, Z. Y.; Qin, B.; Sun, C.; Liu, Y.; Zheng, X.; Zhang, K.; Conney, A. H.; Zeng, H. Q. *Org. Biomol. Chem.* **2012**, *10*, 4164.

(9) As described in entry 8 of Table 2 ($7 + 2\text{CH}_3\text{NH}_2 \rightarrow 7_b \cdot (\text{CH}_3\text{NH}_3^+ + \text{CH}_3\text{NH}_2)$), binding of two amines to neutral 7 is an

exothermic process, releasing a net energy of 1.49 kcal/mol and forming complex $7_b \cdot (\text{CH}_3\text{NH}_3^+ + \text{CH}_3\text{NH}_2)$. This process can be divided into two subprocesses as described in entries 4 and 7 of Table 2. In the first subprocess, neutral 7 binds to the first neutral amine molecule to form $7_b \cdot (\text{CH}_3\text{NH}_3^+)$. According to entry 7 of Table 2, this is an endothermic process, absorbing energy of 3.06 kcal/mol. In the second subprocess, complex $7_b \cdot (\text{CH}_3\text{NH}_3^+)$ can bind to the second neutral amine molecule to form the same complex $7_b \cdot (\text{CH}_3\text{NH}_3^+ + \text{CH}_3\text{NH}_2)$. If the binding of this second amine molecule does not involve any kind of cooperativities, then according to the process described in entry 4 of Table 2, such a binding is also endothermic, needing energy of 3.90 kcal/mol. That is to say, formation of $7_b \cdot (\text{CH}_3\text{NH}_3^+ + \text{CH}_3\text{NH}_2)$ via the two independent processes described in entries 4 and 7 of Table 2 must be an endothermic process, absorbing a total energy of 6.96 kcal/mol (3.06 + 3.90). This is in contradictory to the exothermic process described in entry 8 of Table 2 that forms the same complex from the same set of starting materials (two neutral amine molecules + neutral oligomer 7). Therefore, binding of the two amine molecules to neutral 7 must proceed cooperatively. By determining the difference in energy among these three processes, a positive cooperativity of 8.45 kcal/mol can be estimated.

(10) Zhong, Z.; Li, X.; Zhao, Y. *J. Am. Chem. Soc.* **2011**, *133*, 8862.

(11) Partial assignments of amide signals of 7 and its anionic complexes formed in the presence of amines were made on the basis of 2D $^1\text{H}-^{15}\text{N}$ HMQC and 2D $^1\text{H}-^1\text{H}$ ROESY experiments (Supplementary Figures S4–7). For a better understanding of ^1H NMR of anionic oligomers under basic conditions, two facts need to be noted. (1) Every phenolate anion only causes one of its two adjacent amide protons to downfield shift by >1.5 ppm, suggesting the number of phenolate anions present in any anionic oligomer to be equal to the number of amide protons that are much more downfield shifted than the rest amide protons resonating around 10 ppm; this can be seen from Figure 11 and from other circularly folded anionic pentamers recently reported by us.^{2a} (2) In the presence of strong bases, amide protons may undergo base-mediated hydrogen–deuterium exchange such that some protons cannot be seen in the ^1H NMR spectrum, a reason why 7 in the presence of varying equivalents of TBAOH displays at most 4, rather than 5, amide protons (Figure 11).

(12) Note that the neutral amines cannot compete with the carbonyl O-atoms from anionic 7_{abc} or 7_{abcd} in their interactions with cationic amines since the binding energy involving association of one neutral amine with one cationic amine is 11.22 kcal/mol in THF, a value that is 4.36 and 13.65 kcal/mol less than respective O-atoms at position C in 7_{abc} and 7_{abcd} (Figure 10d,e). Once cationic amines get bound to carbonyl O-atoms, they become unable to further interact with neutral amines due to steric hindrance. Also note that neutral amines do not interact with each other as this H-bond-mediated intermolecular interaction in dimeric or oligomeric amine ensembles (if they do form) leads to a negative binding energy of 0.07 kcal/mol in THF and does not add any stability into the amine molecules.